Dynamic Risk Assessment of Fire-Induced Domino Effects

Chen, Chao; Reniers, Genserik; Yang, Ming

DOI
10.1007/978-3-030-88911-1_2

Publication date
2022

Document Version
Final published version

Published in
Integrating Safety and Security Management to Protect Chemical Industrial Areas from Domino Effects

Citation (APA)
Chen, C., Reniers, G., & Yang, M. (2022). Dynamic Risk Assessment of Fire-Induced Domino Effects. In *Integrating Safety and Security Management to Protect Chemical Industrial Areas from Domino Effects* (pp. 49-68). (Springer Series in Reliability Engineering). Springer. https://doi.org/10.1007/978-3-030-88911-1_2

Chapter 2
Dynamic Risk Assessment of Fire-Induced Domino Effects

2.1 Introduction

In chemical industrial areas,[1] a loss of containment (LOC) of flammable materials can lead to a fire if ignited immediately [4]. Fire is the most common primary scenario of domino effects, accounting for 52.4% of the escalation events in process and storage plants [5]. As a result, many studies have been done to assess fire-induced domino effects, and many safety criteria are based on fire escalation [6]. The International Oil and Gas Producers Association (OGP) provides an escalation threshold of 25 kW/m^2 for the failure of equipment with unprotected steel and 35 kW/m^2 for equipment with cellulosic materials [7]. These thresholds are very simple and user-friendly and thus widely adopted in the engineering domain. However, an assumption that fire propagation is not time-dependent is hidden in threshold-based methods, which may underestimate the likelihood of fire-induced domino effects.

The failure of installations exposed to heat radiation needs to suffer a heat-up process, and the time-lapse between the beginning of exposure and the failure is called time to failure (ttf) [8]. Consequently, the vulnerability of installations exposed to fire depends on both the intensity of heat radiation and the exposure time. For a particular vessel, the ttf decreases with increasing the intensity of heat radiation. Landucci et al. [8] established equations for calculating the ttf of vessels under different intensities of heat radiation. According to the ttf calculation equations and considering the effects of emergency response on preventing fire propagation, probit models are developed to assess the fire-level propagation caused by fire. The probit models are established based on the following assumption: an escalation probability of 0.1 is assumed to be comparable to a ttf equal to 5 min. That of 0.9 is assigned to a ttf equal to 20 min. Since the heat radiation received by installations may change over time and a time-lapse exists between first-level escalation and higher-level escalation, the "probit model" may be unreasonable for accurately estimating the damage probability of

[1] This chapter is mainly based on two publications: Chen et al. [1, 2] and Chen [3].

C. Chen et al., *Integrating Safety and Security Management to Protect Chemical Industrial Areas from Domino Effects*, Springer Series in Reliability Engineering,
https://doi.org/10.1007/978-3-030-88911-1_2

installations in second-level or higher-level propagations. In other words, using the model may result in an overestimation of the probability propagation in secondary or higher levels.

The cause of the primary fire may be accidental events or intentional attacks. The former is related to safety, while the latter involves security. Compared with accidental events, intentional events may be more likely to lead to multiple primary fires due to possible simultaneous attacks on multiple installations. In terms of integrating safety and security, the risk assessment model for fire-induced domino effects should therefore address multiple primary fires.

In a chemical industrial area, various hazardous installations are located nearby with different domino effect potentials. Some installations may have a high probability of initiating domino accidents, while other installations are likely to propagate domino events. Application of graph/ network theory, these installations can be modeled as nodes. The quantitative possibility of accident propagation may be represented by the weight of the edges between nodes in a network or graph [9]. Based on this concept, critical installations contributing to possible domino effects can be identified, and this information may support the allocation of domino prevention resources [10, 11]. This concept can be extended for vulnerability analysis and protection decision-making using graph metrics (e.g., betweenness and closeness) [12–14]. These graph-based models can assess domino risks within an entire industrial area and quickly identify the most critical units. However, they fail to capture the time dependencies and uncertainties in fire escalations. Besides, Bayesian network was also applied to model domino effect propagation [15, 16]. The Bayesian network model can tackle higher-level propagations while it may be difficult to apply it to chemical clusters with a large number of installations [12]. Furthermore, simulation-based approaches were proposed based on the Monte Carlo method to model higher-level propagations. The approach successfully models the spatial evolution of domino accidents, but the shortcoming is obvious, i.e., it is time-consuming [17–20].

In light of the limitations of previous work and the need for integrating safety and security, a dynamic graph approach [1, 2] is introduced in this chapter to model fire escalations, assessing the risk of fire-induced domino effects. Section 2.2 introduces the characteristics of fire escalation, and the theory of dynamic graphs is presented in Sect. 2.3. A domino evolution graph (DEG) model based on dynamic graphs for modeling domino effects triggered by fire is illustrated in Sect. 2.4. Conclusions are drawn in Sect. 2.8.

2.2 Fire Escalation

The majority of escalation events in the chemical and process industry are triggered by fire events such as pool fires and jet fires [21]. These primary scenarios can cause significant heat loads on installations, potentially leading to the failure of process units, storage vessels, pipework, and other target installations through one or more escalation vectors: heat radiation, fire engulfment, and fire impingement [7, 8]. Heat

flux can permeate a vessel wall and lead to the build-up of temperature and pressure within the vessel exposed to the fire. The temperature and pressure of the vessel increase over time and may lead to a loss of containment when the vessel fails. Usually, escalation caused by fire occurs when a loss of containment emerges. If the released hazardous materials are ignited immediately, the damaged tank catches fire and may cause more heat flux on other undamaged vessels nearby. The fire spatially escalates over time. As a result, fire escalation is a spatial–temporal evolution of fire.

2.2.1 Spatial Escalation

Escalation is the main characteristic of domino accidents, linking a primary scenario with one or more than one higher-order scenarios [19]. Based on the spatial escalation characteristics, escalation patterns can be divided into three categories: simple escalation, multilevel domino chain, and multilevel escalation [22], as shown in Fig. 2.1.

(1) Simple escalation: a simple escalation is the domino effect that only a primary scenario triggers a secondary scenario (a "one-to-one" pattern). In the simple escalation, no higher escalations exist, and only two installations are damaged.

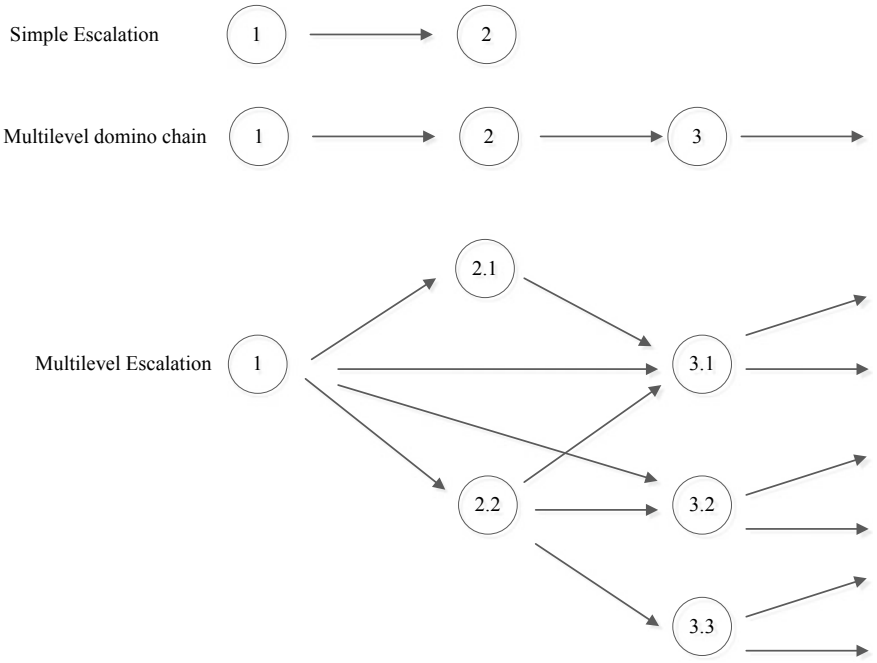

Fig. 2.1 Example of escalation patterns (Chen et al. [1])

(2) Multilevel chain escalation: a multilevel chain escalation consists of a chain of accidents in which a primary scenario triggers a second accident scenario, and the second accident scenario triggers a third accident scenario, and so on. In terms of this pattern, protecting one of the installations in the chain can successfully prevent higher-level escalations.
(3) Multilevel escalation: a multilevel escalation consists of multiple chains. This pattern is a complex pattern in which multiple accident scenarios may trigger one higher-order scenario while multiple accident scenarios can also be induced by one lower-order accident scenario. The former escalation is called the "synergistic effect" while the latter escalation is called the "parallel effect". Due to the two complex effects, modeling multilevel escalations is challenging. As shown in Fig. 2.1, fire at installation 3.1 is triggered by fires at installations 1, 2.1, and 2.2, which is a synergistic effect. The fire at installation 1 induces fires at installations 2.1 and 2.2, which is a parallel effect. The parallel effect shows the escalation capability of an installation to initial and propagate domino effects, while the synergistic effect reflects the vulnerability of an installation. Therefore, the parallel effect and the synergistic effect should be addressed in modeling the spatial escalation of domino effects.

2.2.2 Temporal Escalation

Since there is a time-lapse between the start of exposure and the failure caused by heat radiation, the escalation caused by fire is a time-dependent process. Using a simple escalation (a hazardous material vessel to a hazardous material vessel) as an example, the fire escalation process can be explained as follows:

- The heat caused by a fire is transferred to the vessel wall (shell) by heat radiation or heat convection;
- The target vessel wall is heated, and the temperature rises with the heating;
- The heat transfers from the vessel wall to the liquid and liquid–vapor due to the existing temperature gradients among the vessel wall, the liquid, and the liquid–vapor inside the vessel;
- The internal pressure and temperature of the target vessel increase with the build-up of heat;
- With the heating, the target vessel may fail, resulting in a loss of containment of hazardous materials.

The escalation caused by fire occurs when the target vessel fails. Due to the build-up of heat, the escalation is delayed compared to the time that the target vessel starts to exposure to fire. The time-lapse between the start of the fire and the failure of the target vessel is called "time to failure" (*ttf*) [6]. The burning time of a vessel is called "time to burn out" (*ttb*) [23]. If $ttf < ttb$, then fire escalation may occur; otherwise, the heating ends and the escalation does not occur. Besides the *ttf* and *ttb*, the escalation caused by heat radiation also depends on safety barriers such as

emergency response actions. There is a time-lapse between the start of a fire and the time to control the fire using emergency response. The time-lapse is called "time to control" (*ttc*). Since the escalation of fire depends on multiple temporal factors, it is also a temporal propagation.

According to the characteristics of the escalation induced by fire, a fire-induced domino effect is a spatial–temporal evolution process of fire scenarios in a chemical industrial area. To model fire-induced domino effects, we need to integrate spatial escalation and temporal escalation using a dynamic approach. As a result, a dynamic approach based on graph theory is developed to assess fire-induced domino effects, addressing the spatial–temporal evolution process.

2.3 Graph Theory

2.3.1 Static Graphs

Graph theory is a mathematical method for studying the interconnections between elements in natural and artificial systems. Initially, entity interactions were restricted to binary relationships denoted by graph vertices. Functions were then correlated with graphs, assigning a real number to each graph edge to measure the relationship between any pair of elements in a given graph. A typical graph is made up of a set of vertices (nodes) and edges (arcs), with the assumption that the graph's form is static [2]. A static graph can be an undirected graph, a directed graph, or a weighted graph (network). The three distinct dynamic graph structures are briefly listed below [24–26]:

- An undirected graph is a pair $G = (\mathrm{V}, \mathrm{E})$, where V is a set of vertices, and E is a set of edges. Each edge is an unordered pair where v_{i} and $v_j \in V$;
- A directed graph is a pair $G = (V, A)$, where V is again a set of vertices, and A is a set of arcs. Each arc is an ordered pair (v_i, v_j), $i \neq j$;
- A weighted graph can be represented as $G = (V, E, W_V, W_E)$, where W_V represents the weight of vertices while W_E denotes the weight of edges. The weights can be in different styles: real numbers, complex numbers, integers, elements of some group, etc.

To characterize different graphs, a wide number of metrics were proposed in the literature, such as betweenness, out-closeness, and in-closeness [27]. The betweenness of a vertex v_j is the ratio of the distances between all pairs of other vertexes (v_i and v_k, $i \neq j \neq k$) that traverse v_{j}, to the total distance within the graph, as follows:

$$B_j = \sum_{i,k} \frac{d_{ijk}}{d_{ik}} \tag{2.1}$$

B_j represents the betweenness of vertex v_j; d_{ijk} denotes the distance between vertex v_i and vertex v_k that traverses vertex v_j; d_{ijk} denotes the distance between vertex v_i and vertex v_k that (does not) traverses vertex v_j.

In a directed graph, the closeness of a node v_j can be divided into two types: the out-closeness and the in-closeness. The out-closeness of a vertex v_j depends on the distance needed to reach from the vertex to other vertexes in the graph, as follows:

$$C_{\text{out},j} = \frac{1}{\sum_i d_{ji}} \tag{2.2}$$

$C_{out,j}$ represents the out-closeness of a vertex v_j; d_{ji} denotes the distance of the shortest path from v_j to v_i; The in-closeness of a vertex v_j is determined by the distance needed to reach the vertex from other vertexes in the graph, as follows:

$$C_{\text{in},j} = \frac{1}{\sum_i d_{ij}} \tag{2.3}$$

$C_{in,j}$ denotes the in-closeness of a vertex v_j; d_{ji} denotes the distance of the shortest path from v_i to v_j.

To model different systems, the distance can be defined by different parameters. For instance, d_{ij} may be represented by the ratio between the heat radiation threshold and the actual intensity of heat radiation from installation i to installation j. In that case, d_{ij} represents the escalation potential from installation i to installation j. The escalation potential d_{ij} increases with decreasing the propagation potential from installation i to installation j. The escalation potential of installation i increases with increasing the $C_{out,i}$ and the damage potential of installation i increases with increasing the $C_{in,i}$ [2, 28]. Consequently, graph metrics can be used to identify two types of critical vessels: (i) the critical vessels that have a high potential to initiate a fire-induced escalation and (ii) critical vessels with a high potential to be damaged by domino effects induced by other vessels nearby.

However, the graph metrics based on static graphs can not model the temporal characteristics of fire-induced escalations.

2.3.2 Dynamic Graphs

In real systems, graphs may change over time, such as computer programming languages and artificial intelligence. As a result, dynamic graphs were systematically proposed in the 1990s to model these practical dynamic applications. And some of the static graph algorithms were also improved to study the dynamic systems, such as the shortest path algorithms. A dynamic graph can also be an undirected graph, a directed graph, or a weighted graph. The structure of dynamic graphs is similar to

that of static graphs, while the parameters in a dynamic graph may vary over time [24–26].

A dynamic graph G is updated when one or more of the following four graph parameters change: V (a set of vertexes), E (a set of edges), W_V (map vertexes to numbers), and W_E (map edges to numbers). According to the temporal characteristics, dynamic graphs can be divided into five types:

- Vertex dynamic graph: the set V changes over time, and the vertexes may be added or removed. When a vertex is removed or added, the related edges are also eliminated or increased;
- Edge dynamic graphs: the set E changes over time, and the edges may be added or removed. If an edge is removed or added, the related vertexes may also be deleted or added;
- Vertex weighted dynamic graphs: the weight W_V changes over time and the weights on the nodes update;
- Edge weighted dynamic graphs: the weight W_E changes over time, and the weights on the edge also update;
- Hybrid dynamic graphs: any combination of the above basic types can occur in real applications.

An operation that adds or eliminates vertexes or edges, or changes the weights of vertexes and edges, is referred to as an update on a graph. The graph can be considered unchanged between the two updates. As a result, a dynamic graph can be interpreted as a discrete series of static graphs, and each graph can be analyzed using static graph theory. Dynamic graph models can differ depending on the application, and similar algorithms can be built based on the dynamic graph's update laws [2, 24].

2.4 Domino Evolution Graph Model

Based on the theory of dynamic graphs and the characteristic of spatial–temporal evolution of domino effects, a new domino effect model is proposed in this section.

2.4.1 Dynamic Graph Definition

A Domino Evolution Graph (DEG) is a dynamic graph that represents the spatial–temporal evolution of domino effects triggered by intentional attacks or unintentional events. The DEG starts when there is a primary fire scenario and ends when the escalation is over. In this chapter, only a fire scenario is considered in the model, but it can be extended to model other escalation scenarios such as explosions and toxic dispersions. The DEG can be represented as a hybrid dynamic graph, as follows:

$$DEG = (N,\ E,\ W_N,\ W_E) \tag{2.4}$$

(1) N represents a set of nodes denoting hazardous installations in a chemical industrial area. In this chapter, only the hazardous installations with flammable materials are considered graph nodes since the dynamic graph model only addresses the escalation triggered by fire. The number of nodes (N) is considered unchangeable in the entire evolution process.

(2) E denotes a set of directed edges from installations inducing heat radiation to installations receiving the heat radiation. If an installation j is exposed to heat radiation caused by installation i, the two installations should be linked by a directed edge from node i to node j. Node i is often called tail, while node j is called head ($i \neq j$). An edge can be updated with the evolution of a domino effect.

(3) W_N represents a set of node weights. These weights characterize the vulnerability or harmfulness state of installations, as follows:

$$W_N = (S,\ Q,\ RTF,\ RTB,\ PP,\ PD) \tag{2.5}$$

(i) S represents a set of states that characterize the status of installations in an escalation process. According to the possible roles of hazardous installations in the evolution of fire-induced domino effects, three installation states are defined: "vulnerable", "harmful" and "failed". The description of these states is shown in Table 2.1. To better display the state of installations in a graph, installations in the "vulnerable" state are marked as yellow, those in the "harmful" state are marked as red, and those in the "failed" state are marked as gray in the dynamic graph. An escalation occurs when an installation in a "vulnerable state" transfers to a "harmful" state.

(ii) Q represents the total heat radiation received by installations, in kW/m^2. Only installations in the "vulnerable" state receive heat radiations from installations in a "harmful" state. The Q of installations in a "harmful" state or a "failed" state is considered to be zero.

Table 2.1 State descriptions (Chen et al. [2])

State	Description	Marked color
Vulnerable	The installation is not physically damaged, but it may receive heat radiation from other installations. The installation's temperature or internal pressure may increase in this state	Yellow
Harmful	The installation is on fire due to intentional events or due to escalation from other installations. Installations in this state have a harmful impact on other installations receiving their heat radiation	Red
Failed	The fire on the installation is extinguished due to the burning out of flammable substances or emergency response actions. All edges connected to the node will be removed if the installation's state transfers from "harmful" to "failed"	Gray

(iii) *RTF* denotes the residual time to failure (*RTF*) of installations in the "vulnerable" state, in min. *RTF* is equal to zero when an installation is damaged while it is assumed to be infinite when an installation is in the "failed" state.

(iv) *RTB* represents the residual time to burn out (*RTB*) of installations in the "harmful" state, in min. An installation in a "harmful" state transfers to a "failed" state when *RTB* is equal to zero.

(v) *PP* represents the probabilities of primary fire on installations. It denotes the vulnerability of installations directly against unintentional or intentional events. The *PP* may be decreased by improving the resistant capability of installations using safety and security measures. The likelihood of installations being damaged by domino effects is not considered in the weight.

(vi) W_E represents the weight of directed edges. It only consists of one weight: the heat radiations from tail installations to head installations, kW/m^2. The W_E can be represented by a square matrix of dimension $N \times N$ (an adjacent matrix), as follows:

$$EW = \begin{bmatrix} 0 & q_{12} & \dots & q_{1n} \\ q_{21} & 0 & \dots & q_{2n} \\ \dots & \dots & 0 & \dots \\ q_{n1} & q_{n2} & \dots & 0 \end{bmatrix} \tag{2.6}$$

where q_{ij} denotes the heat radiation intensity caused by installation i in the "harmful" state to installation j in the "vulnerable" state. q_{ij} is equal to zero when there is no directed edge from installation i to installation j. In the adjacent matrix, row i indicates the escalation potential of installation i, and column j represents the vulnerability of installation j.

2.4.2 Dynamic Graph Update

(1) **Evolution update**

A Domino Evolution Graph (DEG) consists of a chain of static graphs. The initial static graph (Graph 1) emerges when a primary scenario caused by unintentional or intentional events occurs. A new static graph will occur if an update operation is conducted. The graph index (g) is also updated according to the operation, as follows:

$$g = \begin{cases} 1 & \text{initial graph} \\ g+1 & \text{after a new update} \end{cases} \tag{2.7}$$

The time between two update operations is called "graph time" t (min). The evolution time at the beginning of graph g (T_g) can be obtained, as follows:

Fig. 2.2 State transition of installations (Chen et al. [2])

$$T_g = \begin{cases} 0 & g = 1 \\ T_{g-1} + t_{g-1} & g > 1 \end{cases} \tag{2.8}$$

(2) **State update**

Among the three installation states, update operations can be divided into two types: from "vulnerability" to "harmful" and from "harmful" to "failed", as shown in Fig. 2.2. In the first graph, the installations on fire are in the "harmful" state, and other installations are in the "vulnerable" state. If an installation is damaged and on fire due to escalation from external installations, its state will be changed from "vulnerable" to "harmful". Furthermore, if the fire on an installation is extinguished, the installation will be updated to a "failed" state. Finally, the update operation will terminate if no escalation occurs in which no installation is in the "vulnerable" state, and no installation is in the "harmful" state.

(3) **Directed edge update**

Directed edges link "harmful" installations with "vulnerable" installations. As a result, when the state of an installation is changed, the directed edges should be added or removed. When an installation's state changes to "harmful," all directed edges from other installations to the installation will be removed while all directed edges from the installation to other installations will be established. If an installation's state changes to "failed" the directed edges from (to) that installation to (from) other installations are erased.

(4) **Heat radiation update**

In a domino effect evolution process, installations with a "vulnerable" state can obtain heat radiations from more than one installation with "harmful" states, a phenomenon which is known as "synergistic effect". In contrast, an installation in the "harmful" state can emit heat to several installations in the "vulnerable" state, which is called "parallel effects". Figure 2.3a depicts a graph model of a parallel effect while Fig. 2.3b depicts a graph model of a synergistic effect.

Due to the synergistic effect, the total heat radiation suffered by an installation j in the "vulnerable state" (Q_j) should be the sum of heat radiations received from other installations in "harmful" states, as follows:

$$Q_j = \sum_{i=1}^{N} q_{ij} \tag{2.9}$$

The total amount of heat radiation obtained by each installation may change over time due to new occurrences of "harmful" installations or "failed" installations. The

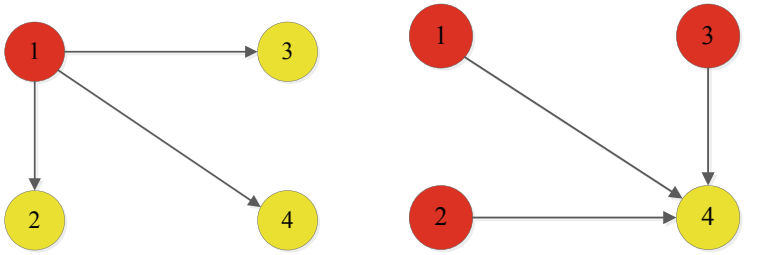

(a) Parallel (divergence) effects (b) Synergistic (convergence) effects

Fig. 2.3 Graph models of the spatial evolution of domino effects (Chen et al. [2])

heat radiation from installation i in the "harmful" state to installation j in the "vulnerable" state can be calculated by the application of consequence analysis software such as ALOHA [29].

(5) **Residual time to failure update**

Because of superimposed effects, the *RTF* of installations in "vulnerable" states may change over time in a domino effect evolution. Besides, passive protection measures such as fireproof coatings, have an impact on the *RTF*. When an installation j starts receiving heat radiation at evolution time T_g, the *RTF* can be obtained without considering the superimposed effect, as follows [8]:

$$RTF_{j,g} = \frac{\exp\left(c_1 \times V^{c_2} + c_3 \ln(Q_j) + c_4\right)}{60} \tag{2.10}$$

$RTF_{j,g}$ represents the residual time to failure of installation j at T_g (min); c_1–c_4 are parameters related to vessel factors, as shown in Table 2.2.

If $RTF_{j,g} < t_g$, the installation j will be physically damaged and escalation will occur at T_{g+1}. Otherwise, the *RTF* of installation j in the "vulnerable" state at the time T_{g+1} will be updated according to superimposed effects: the heat radiation in different stages received by the installation should be superimposed to calculate the *RTF* at the time of T_{g+1}, as follows [1]:

$$RTF_{j,g+1} = \left(\frac{Q_{j,g+1}}{Q_{j,g}}\right)^c \cdot \left(RTF_{j,g} - t_g\right) \tag{2.11}$$

(6) **Residual time to burn out update**

Table 2.2 The parameter value of a, b, c, and d (Landucci et al. [8])

Installation	c_1	c_2	c_3	c_4
Atmospheric tank	-2.67×10^{-5}	1	−1.13	9.9
Pressurized tank	8.845	0.032	−0.95	0

Given that an installation i is on fire at the time of T_g, RTB of the installation at that time can be obtained as the ratio of flammable material mass to burning rate, as follows:

$$RTB_{i,\,g} = \frac{m_i}{v_i} \tag{2.12}$$

m_i represents the mass of flammable substances in installation i (kg); v_i represents the burning rate of flammable substances in installation i (kg/min); $RTB_{i,\,g}$ denotes the RTB of installation i at the evolution time of T_g.

If $RTB_{j,\,g} < t_g$, the installation i will be extinguished; otherwise, it will continue to be on fire at $T_{g+1,}$ and the RTB of installation i at T_{g+1} will be updated, as follows:

$$RTB_{i,\,g+1} = RTB_{i,\,g} - t_g \tag{2.13}$$

(7) **Escalation probability update**

In the chemical industry, emergency response is critical for preventing escalation or for mitigating domino effects [30]. As a result, emergency management should be considered when assessing the risk of plant installations. However, due to the complexities associated with human factors in executing emergency response activities, evaluating emergency response is very difficult. For the sake of simplicity, we assume that the domino effect progression can not be prevented until the emergency mitigation steps are effectively initiated [8]. In this chapter, a cumulative log-normal distribution (LND) function is used to model the time required to control domino effects (TTC) by emergency response actions, as follows:

$$\log TTC \sim N\left(u, \sigma^2\right) \tag{2.14}$$

u represents the mean of log TTC or expectation of the distribution; σ denotes the standard deviation of log TTC and σ^2 represents the variance. Maximum Likelihood Estimation (MLE) can be used to calculate these factors based on expert judgment, disaster drills, or models. Consequently, if an installation j is supposedly damaged at T_g with a certain probability during a domino effect evolution, the conditional probability of installation j being damaged (PD) given a primary scenario can be obtained, as follows:

$$P_{d,j} = \left(1 - \mathrm{LND}\left(T_g\right)\right) \tag{2.15}$$

2.5 Algorithm

The Domino Evolution Graph (DEG) model is developed in Sect. 2.4. This section introduces the Minimum Evolution Time (MET) algorithm [1] to solve the DEG model, as shown in Fig. 2.4. According to the algorithm, First, basic data needed for risk assessment of domino effects caused by fire need to be inputted, such as chemical plant layout information, potential heat radiations calculated by ALOHA software, and primary fire scenarios. Next, the parameters of the DEG model should be initialized given the primary fire scenario. Then, the *RTF* and *RTB* of each installation should be estimated according to the methods illustrated in Sect. 2.4. The initial DEG is updated when the evolution time is equal to the minimum value (t_m) of *RTF* and *RTB*, as follows:

$$t_m = \min(RTB_i, RTF_j)\, i, j = 1, 2, \ldots n \tag{2.16}$$

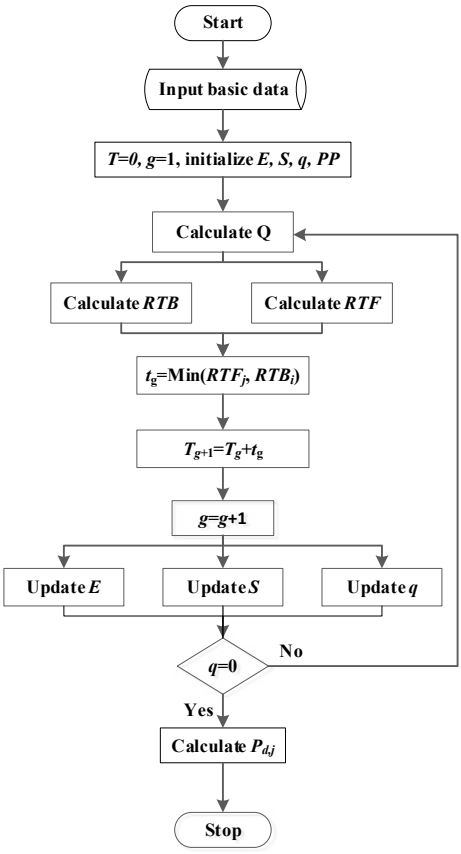

Fig. 2.4 Flow diagram of the MET algorithm for the DEG model (Chen et al. [2])

The parameters of E, S, q, and T are updated accordingly. The above steps will continue until q is equal to zero. Then, the graph update will terminate and the damage probability of each installation is calculated based on emergency response information. According to the algorithm, we can rapidly obtain the graph time, installation states at each time, the damage probability of installations, and the likelihood of domino effects.

2.6 Case Study

Figure 2.5 shows an illustrative chemical plant consisting of four storage tanks. The characteristics of these tanks are summarized in Table 2.3. The meteorological parameters of the chemical plant are assumed as follows: an ambient temperature of 20°C, the wind blowing from the West with a speed of 1.5 m/s, relative humidity of 50%, and the stability class D. The heat radiation intensity generated by a pool fire and the burning rate of each fire are calculated by the ALOHA software, as shown in Table 2.4. Assuming u is equal to 10 min and the corresponding variance is equal to 2 min [1].

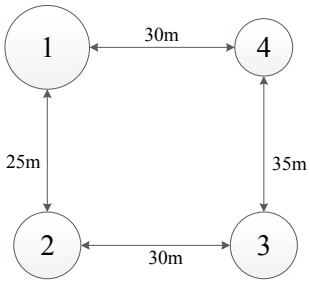

Fig. 2.5 Layout of an illustrative chemical plant (Chen et al. [2])

Table 2.3 Features of chemical storage tanks (Chen et al. [2])

Tank	Type	Dimension	Chemical substance	Volume (m^3)	Chemical content (t)
1	Atmospheric	30 × 10	Benzene	6000	4000
2	Atmospheric	20 × 10	Acetone	2500	2000
3	Atmospheric	20 × 10	Toluene	2500	1500
4	Atmospheric	10 × 6.5	Toluene	500	200

Table 2.4 The Heat Radiation from tank *i* to tank *j* and the *ttb* of tanks (Chen et al. [2])

Tank *i*, *j*	q_{ij} (kW/m^2)				*ttb* (min)
	1	2	3	4	
1	–	32.5	25.1	12.9	1666.7
2	17.7	–	13.2	4.1	1369.9
3	8.7	17.6	–	13.8	980.4
4	10.1	3.5	8.3	–	233.9

2.6.1 The Application of Graph Metric Approach

Using the static graph methodology, setting a threshold value of 15 kW/m^2, a static graph of the chemical plant is obtained, as shown in Fig. 2.6. The calculation results of the graph metrics (e.g., out-closeness and in-closeness) of the four tanks are listed in Table 2.5.

According to the out-closeness results illustrated in Table 2.5, Tank 1 has the highest potential to initiate a fire-induced domino effect if it is on fire, followed by Tank 2 and then Tank 3. The fire at Tank 4 can not trigger a domino effect. Based on the in-closeness value, Tank 2 is most vulnerable to domino effects, followed by Tank 3, and also Tank 1. Tank 4 is more likely not to fail when a domino effect occurs at one of the other tanks in the chemical plant.

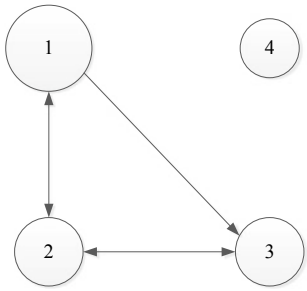

Fig. 2.6 Static graph model of the chemical plant (Chen et al. [2])

Table 2.5 The results of closeness for the static graph in Fig. 2.7 (Chen et al. [2])

Tank	Out-closeness	In-closeness
1	0.42	0.17
2	0.19	0.34
3	0.17	0.22
4	0	0

Table 2.6 The damage time of tanks (min) (Chen et al. [2])

Tank	S1	S2	S3	S4	S5
1	0	11.0	19.2	–	0
2	6.1	0	12.2	–	0
3	7.4	16.1	0	–	5.1
4	13.5	20.3	22.2	0	9.3

2.6.2 The Application of Dynamic Graph Approach

According to the dynamic graph approach, five primary scenarios are assumed, as follows: (S1) Pool fire at Tank 1; (S2) Pool fire at Tank 2; (S3) Pool fire at Tank 3; (S4) Pool fire at Tank 4; (S5) Pool fires at Tank 1 and Tank 2. Using the dynamic graph approach, the failure time of each tank caused by different primary scenarios can be estimated, as shown in Table 2.6.

Taking primary scenario 2 as an example, Tank 1 is on fire at $T = 0$ min (Fig. 2.7a). The heat radiation emitted from Tank 2 can cause credible damage to tanks 1, 3, and

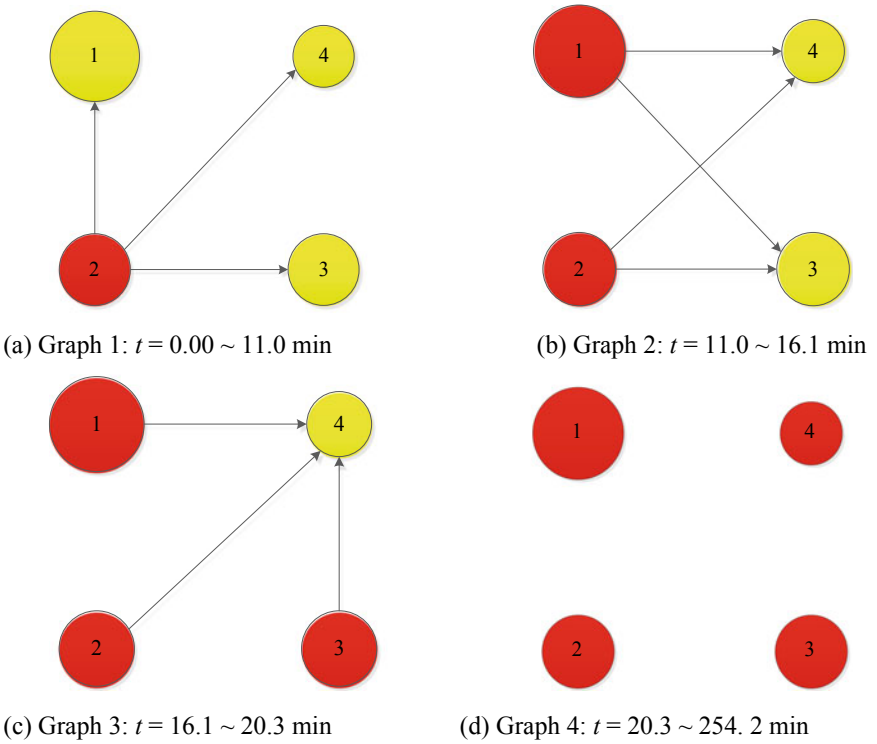

(a) Graph 1: $t = 0.00 \sim 11.0$ min

(b) Graph 2: $t = 11.0 \sim 16.1$ min

(c) Graph 3: $t = 16.1 \sim 20.3$ min

(d) Graph 4: $t = 20.3 \sim 254.2$ min

Fig. 2.7 The DEG caused by a fire at tank 2 (Chen et al. [2])

Table 2.7 The conditional probability of tanks being damaged (Chen et al. [2])

Tank	A1	A2	A3	A4	A5	PBD
1	1.00	0.23	1.34×10^{-6}	0	1.00	0.45
2	1.00	1.00	0.07	0	1.00	0.61
3	0.98	2.95×10^{-4}	1.00	0	1.00	0.60
4	0.01	1.70×10^{-7}	4.91×10^{-9}	1.00	0.68	0.34
PCD	0.75	0.31	0.27	0.25	–	–

4, leading to a fire at Tank 1 at $T = 11.0$ min. In that case, the state of Tank 1 transfers from "vulnerable" to "harmful", leading to a synergistic effect on Tank 3 and Tank 4, as shown in Fig. 2.7b. Then, Tank 3 is on fire at $T = 16.1$ min (Fig. 2.7c) due to the synergistic effect and a superimposed effect caused by Graph 1 and Graph 2. Finally, Tank 4 catches fire at $T = 20.3$ min.

Considering the uncertainty of emergency response according to Eq. (2.14), we can obtain the damage probability of each Tank of different primary scenarios, as shown in Table 2.7. It indicates that the domino effect caused by the attack on Tank 1 may be inevitable due to the fastest evolution. Tank 2 with the highest average conditional probability of being damaged (PBD) is more susceptible to domino effects caused by other tanks. While Tank 1 has the highest potential to initiate domino effects since it has the largest value of the average conditional probability to cause damage (PCD).

2.7 Discussion

In this study, we introduced the static graph method and the dynamic graph method for modeling fire-induced domino effects. According to the results of a case study, the ranking of tanks based on their in-closeness values is the same as their ranking based on their average conditional probability of being damaged (PBD). Besides, the ranking of tanks based on their out-closeness is also identical to their ranking based on their average conditional probability to cause damage (PCD). Therefore, It may be demonstrated that the DEG model proposed in this chapter is valid. Moreover, The dynamic graph approach can obtain the dynamic evolution of domino effects compared to the static graph which seems to provide merely a snapshot of the whole process at once.

This study develops the Minimum Evolution Time (MET) algorithm to solve the DEG model, avoiding the time-consuming approach of repeatedly generating random numbers. The maximum number of iterations of the MET algorithm is $2n$ while the minimum number of iterations of Monte Carlo-based simulation tools is 10^4–10^6 [17, 20]. So the calculation efficiency is improved greatly. As a result, this approach can be used for assessing fire-induced domino effects in chemical clusters with a large number of hazardous installations.

In the DEG model, an adjacent matrix is used to represent potential heat radiations between each pair of tanks. In that case, the primary scenario with multiple fires that is more likely to be induced by multiple attacks can be addressed. As shown in Table 2.6, both Tank 1 and Tank 2 are on fire in primary scenario 5, leading to a faster evolution than the primary scenarios with single fires (S1, S2, S3, S4, and S5) and making the prevention of a domino effect more difficult. Besides, parallel effects, synergistic effects, and superimposed effects can also be considered in this model.

In this chapter, we only consider fire and neglect vapor cloud explosion (VCE) in domino effects. The next chapter will model domino effects triggered by VCEs.

2.8 Conclusions

This chapter introduces a Domino Evolution Graph (DEG) model and a Minimum Evolution Time (MET) algorithm to model the spatial–temporal evolution of domino effects triggered by fires. The evolution process is divided into stages according to chronological order. A series of static graphs representing a domino evolution process is sequentially connected by superimposed effects, constituting a DEG. To rapidly solve the DEG model, the MET algorithm based on the principle of minimum evolution time is developed. By applying the MET algorithm, we can obtain the evolution graphs, evolution time, evolution probability, escalation probability, and the damage probability of each installation exposed to fire-induced domino effects. Compared with graph metrics, the DEG model can grasp the dynamic evolution characteristics of domino effects and overcome the limitation of the "probit model" in higher-level escalations. The developed model can be applied to support the decision-making on safety and security barriers since it can be used in real chemical plants and chemical clusters with a large number of hazardous installations. Besides, this approach can also be extended to domino effect assessment related to multi-hazard accident scenarios (fire, explosion, and toxic release).

References

1. Chen C, Reniers G, Zhang L (2018) An innovative methodology for quickly modeling the spatial-temporal evolution of domino accidents triggered by fire. J Loss Prev Process Ind 54:312–324
2. Chen C, Reniers G, Khakzad N (2019) Integrating safety and security resources to protect chemical industrial parks from man-made domino effects: a dynamic graph approach. Reliab Eng Syst Saf 191
3. Chen C (2021) A dynamic and integrated approach for modeling and managing domino-effects. Delft University of Technology
4. Chen C, Khakzad N, Reniers G (2020) Dynamic vulnerability assessment of process plants with respect to vapor cloud explosions. Reliab Eng Syst Saf 200
5. Darbra RM, Palacios A, Casal J (2010) Domino effect in chemical accidents: main features and accident sequences. J Hazard Mater 183(1–3):565–573

6. Necci A, Cozzani V, Spadoni G, Khan F (2015) Assessment of domino effect: state of the art and research needs. Reliab Eng Syst Saf 143:3–18
7. Alileche N, Cozzani V, Reniers G, Estel L (2015) Thresholds for domino effects and safety distances in the process industry: a review of approaches and regulations. Reliab Eng Syst Saf 143:74–84
8. Landucci G, Gubinelli G, Antonioni G, Cozzani V (2009) The assessment of the damage probability of storage tanks in domino events triggered by fire. Accid Anal Prev 41(6):1206–1215
9. Reniers GLL, Dullaert W (2007) DomPrevPlanning©: User-friendly software for planning domino effects prevention. Saf Sci 45(10):1060–1081
10. Reniers G, Dullaert W, Audenaert A, Ale BJ, Soudan K (2008) Managing domino effect-related security of industrial areas. J Loss Prev Process Ind 21(3):336–343
11. Zhang X, Chen G (2011) Modeling and algorithm of domino effect in chemical industrial parks using discrete isolated island method. Saf Sci 49(3):463–467
12. Khakzad N, Reniers G (2015) Using graph theory to analyze the vulnerability of process plants in the context of cascading effects. Reliab Eng Syst Saf 143:63–73
13. Khakzad N, Reniers G, Abbassi R, Khan F (2016) Vulnerability analysis of process plants subject to domino effects. Reliab Eng Syst Saf 154:127–136
14. Khakzad N, Reniers G, van Gelder P (2017) A multi-criteria decision making approach to security assessment of hazardous facilities. J Loss Prev Process Ind 48:234–243
15. Khakzad N, Khan F, Amyotte P, Cozzani V (2013) Domino effect analysis using Bayesian networks. Risk Anal 33(2):292–306
16. Khakzad N (2015) Application of dynamic Bayesian network to risk analysis of domino effects in chemical infrastructures. Reliab Eng Syst Saf 138:263–272
17. Zhang L, Landucci G, Reniers G, Khakzad N, Zhou J (2017) DAMS: a model to assess domino effects by using agent-based modeling and simulation. Risk Anal
18. Zhou J, Reniers G (2016) Petri-net based simulation analysis for emergency response to multiple simultaneous large-scale fires. J Loss Prev Process Ind 40:554–562
19. Zhou J, Reniers G, Khakzad N (2016) Application of event sequence diagram to evaluate emergency response actions during fire-induced domino effects. Reliab Eng Syst Saf 150:202–209
20. Abdolhamidzadeh B, Abbasi T, Rashtchian D, Abbasi SA (2010) A new method for assessing domino effect in chemical process industry. J Hazard Mater 182(1–3):416–426
21. Gómez-Mares M, Zárate L, Casal J (2008) Jet fires and the domino effect. Fire Saf J 43(8):583–588
22. Reniers G, Cozzani V (2013) Domino effects in the process industries, modeling, prevention and managing. Elsevier, Amsterdam
23. Khakzad N, Khan F, Amyotte P, Cozzani V (2014) Risk management of domino effects considering dynamic consequence analysis. Risk Anal 34(6):1128–1138
24. Harary F, Gupta G (1997) Dynamic graph models. Math Comput Model 25(7):79–87
25. Bondy JA, Murty USR (1976) Graph theory with applications, vol 290. Citeseer
26. Casteigts A, Flocchini P, Quattrociocchi W, Santoro N (2012) Time-varying graphs and dynamic networks. Int J Parallel Emergent Distrib Syst 27(5):387–408
27. Hernández JM, Van Mieghem PJDUoTM, The Netherlands (2011) Classification of graph metrics 1–20
28. Khakzad N (2018) A graph theoretic approach to optimal firefighting in oil terminals. Energies 11(11)

29. ALOHA user manual (2016) US Environmental Protection Agency, National Oceanic and Atmospheric Administration, ALOHA, Version 5.4.7. https://www.epa.gov/cameo/aloha-software. Accessed 5 May 5 2019
30. Zhou J, Reniers G (2016) Petri-net based modeling and queuing analysis for resource-oriented cooperation of emergency response actions. Process Saf Environ Prot 102:567–576